

## DESIGN AND ANALYSIS OF GAS TURBINE ROTOR BLADE USING FINITE ELEMENT METHOD

AHMED ABDULHUSSEIN JABBAR<sup>1</sup>, A. K. RAI<sup>2</sup>, P. RAVINDER REEDY<sup>3</sup> & MAHMOOD HASAN DAKHIL<sup>4</sup>

<sup>1,2,4</sup>Department of Mechanical Engineering, SHIATS -DU, Allahabad, India

<sup>3</sup>Department Professor & Head of Mechanical Engineering. Chaitanya Bharathi Institute  
of Technology, Hyderabad, Andhra Pradesh, India

### ABSTRACT

In the present work the first stage rotor blade of a two-stage gas turbine has been analyzed for structural, thermal using ANSYS 12 which is powerful Finite Element Software. In the process of getting the thermal stresses, the temperature distribution in the rotor blade has been evaluated using this software. From different materials titanium alloy, stainless steel alloy and Aluminum2024 alloy that has been considered for the purpose analysis. . The turbine blade along with the groove is considered for the static, thermal, modal analysis. The blade is modeled with the 3D-Solid Brick element. The geometric model of the blade profile is generated with splines and extruded to get a solid model. It is observed that the Maximum temperatures are observed at the blade tip section are linearly decreasing from the tip of the blade to the root of the blade section.

**KEYWORDS:** Gas Turbine, Structural Analysis, Thermal Analysis, Modal, Finite Element Analysis

### INTRODUCTION

#### General

The purpose of turbine technology are to extract the maximum quantity of energy from the working fluid to convert it into useful work with maximum efficiency by means of a plant having maximum reliability, minimum cost, minimum supervision and minimum starting time. The gas turbine obtains its power by utilizing the energy of burnt gases and the air which is at high temperature and pressure by expanding through the several rings of fixed and moving blades. To get a high pressure of order 4 to 10 bar of working fluid where fuel is continuously burnt with compressed air to produce a steam of hot, fast moving gas as shown in figure 1 [1].

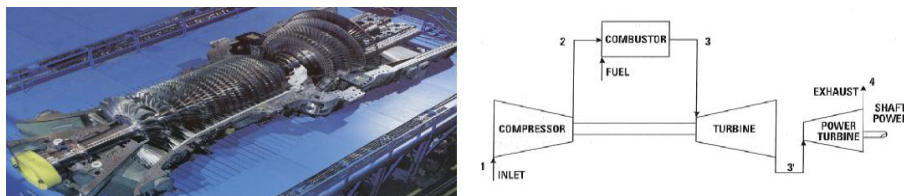


Figure 1: Gas Turbine Simple Open Cycle

This gas stream is used to power the compressor that supplies the air to the engine as well as providing excess energy that may be used to do other work, which is essential for expansion a compressor, is required. The quantity of the working fluid and speed required are more so generally a centrifugal or an axial compressor is required. The turbine drives the compressor so it is coupled to the turbine shaft. If after compression the working fluid were to be expanded in a turbine, then assuming that there were no losses in either component, the power developed by the turbine can be increased by increasing the volume of working fluid at constant pressure or alternatively increasing the pressure at constant volume.

Either of these may be done by adding heat so that the temperature of the working fluid is increased after compression. To get a higher temperature of the working fluid a combustion chamber is required where combustion of air and fuel takes place giving temperature rise to the working fluid. Gas turbines have been constructed to work on the following: -oil, natural gas, coal gas, producer gas, blast furnace and pulverized coal.

The engine consists of three main parts.

- The Compressor section
- The Combustion section (the combustor).
- The turbine (and exhaust) section.

The Turbine compressor usually sits at the front of the engine. There are two main types of compressor, the centrifugal compressor and the axial compressor. The compressor will draw in air and compress it before it is fed into the combustion chamber. In both types, the compressor rotates and it is driven by a shaft that passes through the middle of the engine and is attached to the turbine as shown below in figure 2 [1], [2].

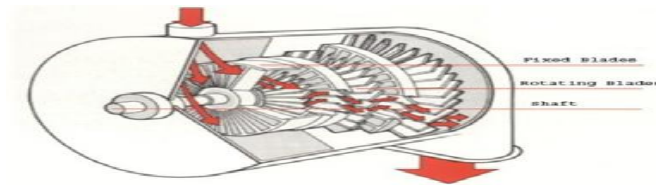


**Figure 2: Turbine Blade Coupled to Centrifugal Compressor**

### Types of Gas Turbine

There are four main types of gas turbine: The turbojet, turbofan, turboprop and turbo shaft[2].

### Fuel for Gas Turbine Power Plants

Gas turbine fuel systems are similar for all Turbines. For the most common fuels, which are natural gas, LNG (liquid natural gas), and light diesel, the fuel system consists:

A fuel delivery system, Fuel nozzles, Fuel additives (to deal with vanadium), Fuel washing (to deal with sodium and potassium Salts) and Modifications to the fuel delivery system[3].

### Natural Gas

Natural gas comprises over 80% methane with minor amounts of ethane, propane, butane, and heavier hydrocarbons. It may also include carbon dioxide, nitrogen, and hydrogen. There are a plethora of blends of natural gas available worldwide[3].

### Applications of Gas Turbine

The following are the applications of gas turbine as shown in figure 3.

- **Land Applications:** Central power stations, Industrial and Industrial.
- **Space Applications:** Turbo jet and Turbo prop.
- Marine application [1].



**Figure 3: Some Examples of Application Gas Turbine**

### Turbine Blade

The rotor blades of the turbo machine are very critical components and reliable operation of the turbo machine as a whole depends on their repayable operation. The major cause of break down in turbo machine is the failure of rotor blade. The failure of the rotor blade may lead to catastrophic consequences both physically and economically. Hence, the proper design of the turbo machine blade plays a vital role in the proper functioning of the turbo machine as shown in figure 4[1].



**Figure 4: Turbine Blade**

A good design of the turbo machine rotor blading involves the following:

- Determination of geometric characteristics from gas dynamic analysis.
- Determination of steady loads acting on the blade and stressing due to them.
- Determination of natural frequencies and mode shapes.
- Determination of unsteady forces due to stage flow interaction.
- Determination of dynamic forces and life estimation based on the cumulative damage fatigue theories[3].

### Production of Blades

Blades may be considered to be the heart of turbine and all other member exist for the sake of the blades. Without blade there would be no power and the slightest fault in blade would mean a reduction in efficiency and costly repairs. The following are some of the methods adopted for production of blades.

- **Rolling:** Sections are rolled to the finished size and used in conjunction with packing pieces. Blades manufactured by this method do not fail under combined bending and centrifugal force.
- **Machining:** Blades are also machined from rectangular bars. This method has more or less has the same advantage as that of first. Impulse blade is manufactured by this technique.
- **Forging:** Blade and vane sections having airfoil sections are manufactured by specialist techniques.
- **Extrusion:** Blades are sometimes extruded and the roots are left on the subsequent machining. This method is not reliable as rolled sections, because of narrow limits imposed on the composition of blade material [4].

## Turbine Blade Cooling

Unlike steam turbine bladings, gas turbine bladings need cooling. The objective of the blade cooling is to keep the metal temperature at a safe level to ensure a long creep life and low oxidation rates. Although it is possible to cool the blades by liquid using thermosyphon and heat pipe principal, but the universal method of blade cooling is by cool air or working fluid flowing through internal passage in the blades. The mean rotor blade temperature is about  $350^{\circ}\text{C}$  below the prevailing gas temperature after efficient blade cooling as shown below in figure 5.

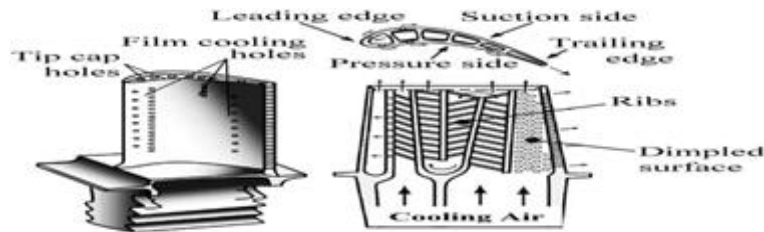


**Figure 5: Turbine Blades Cooling**

Due to corrosion and corrosion deposits turbine blades fail. To protect it from corrosion, the uses of pack-aluminized coatings are used. The main elements used are aluminum, nickel, and chromium[1], [5].

## ASSUMPTION SYSTEM AND SIMULATIONS

### Turbine Blade Materials

Advancements made in the field of materials have contributed in a major way in building gas turbine engines with higher power ratings and efficiency levels. Improvements in design of the gas turbine engines over the years have importantly been due to development of materials with enhanced performance levels. Gas turbines have been widely utilized in aircraft engines as well as for land based applications importantly for power generation. Advancements in gas turbine materials have always played a prime role – higher the capability of the materials to withstand elevated temperature service, more the engine efficiency; materials with high elevated temperature strength to weight ratio help in weight reduction. A wide spectrum of high performance materials - special steels, titanium alloys and super alloys - is used for construction of gas turbines [4]. The material available limits the turbine entry temperature (TET). The properties required are as follows (a) tensile strength (b) resistance to high frequency vibration fatigue stresses (c) low frequency thermal fatigue stresses (d) resistance to erosion and corrosion [1].

### Stainless Steel Alloy

In spite of this there is a group of iron-base alloys, the iron-chromium-nickel alloys known as stainless steels, which do not rust in sea water, are resistant to concentrated acids and which do not scale at temperatures up to  $1100^{\circ}\text{C}$ . It is this largely unique universal usefulness, in combination with good mechanical properties and manufacturing characteristics, which gives the stainless steels their *raison d'être* and makes them an indispensable tool for the designer. The usage of stainless steel is small compared with that of carbon steels but exhibits a steady growth, in contrast to the constructional steels. Stainless steels as a group is perhaps more heterogeneous than the constructional steels, and their properties are in many cases relatively unfamiliar to the designer. In some ways stainless steels are an unexplored world but to take advantage of these materials will require an increased understanding of their basic properties[6].

### Titanium Alloy

These titanium alloys are mainly used for substituting materials for hard tissues. Fracture of the alloys is, therefore, one of the big problems for their reliable use in the body. The fracture characteristics of the alloys are affected by

changes in microstructure. Therefore, their fracture characteristics, including tensile and fatigue characteristics should be clearly understood with respect to microstructures. The fracture characteristics in the simulated body environment also be identified because the alloys are used as biomedical materials. The effect of living body environment on the mechanical properties is also very important to understand.

**Alpha Structure ( $\alpha$  Alloy):** with alpha stabilizer elements present, these alloys possess excellent creep resistance. They are also used largely in cryogenic applications.

**Alpha Beta Structure ( $\alpha$ - $\beta$  Alloy):** this group contains both alpha and beta stabilizer elements. This is the largest group in the aerospace industry.

**Beta Structure ( $\beta$  Alloy):** with beta stabilizers this group has high harden ability and high strength, but also a higher density. Titanium alloys use in aero engines, Automotive, Airframes and road transport, Dental alloys, geothermal plant, Marine and Military hardware[7].

**Aluminum Alloy**

The production of primary aluminum is a young industry - just over 100 years old. But it has developed to the point where scores of companies in some 35 countries are smelting aluminum and thousands more are manufacturing the many end products to which aluminum is so well suited. Alloy A380 (ANSI/AA A380.0) is by far the most widely cast of the aluminum die-casting alloys, offering the best combination of material properties and ease of production. It may be specified for most product applications. Aluminum Alloys use in Electrical Conductors, Transport, Packaging, and High Pressure Gas Cylinders [4].

**Table 1: Material Properties [8]**

Properties	Units	Titanium Alloy	Stainless Steel Alloy	Aluminum 2024 Alloy
Density	kg/m <sup>3</sup>	4700	8025	2725
Thermal conductivity(K)	W/m.k <sup>0</sup>	10	33.5	180
Coefficient of thermal expansion( $\alpha$ )	C <sup>0</sup>	8.8	14.5	23.3
Specific heat (CP)	J/kg.K <sup>0</sup>	544	448	880
Modules of elasticity (E)	GPa	205	200	73
Poisson ratio( $\mu$ )	.....	0.33	0.3	0.33
Melting point	<sup>0</sup> C	1649	1451	565
Ultimate tensile strength	MPa	1000	1050	470

**Finite Element Method**

The finite element method (FEM) has now become a very important tool of engineering analysis. Its versatility is reflected in its popularity among engineers and designers belonging to nearly all the engineering disciplines. Whether a civil engineer designing bridges, dams or a mechanical engineers designing auto engines, rolling mills, machine tools or an aerospace engineer interested in the analysis of dynamics of an aero plane or temperature rise in the heat shield of a space shuttle or a metallurgist concerned about the influence of a rolling operation on the microstructure of a rolled product or an electrical engineer interested in analysis of the electromagnetic field in electrical machinery-all find the finite element method handy and useful[9]. It is not that these problems remained unproved before the finite element method came into vogue; rather this method has become popular due to its relative simplicity of approach and accuracy of results. Traditional methods of engineering analysis, while attempting to solve an engineering problem mathematically, always try for simplified formulation in order to overcome the various complexities involved in exact mathematical formulation. In the

modern technological environment the conventional methodology of design cannot compete with the modern trends of Computer Aided Engineering (CAE) techniques [10]. The constant search for new innovative design in the engineering field is a common trend. To build highly optimized product, this is the basic requirement of today for survival in the global market. All round efforts were put forward in this direction. Software professional and technologists have developed various design packages [11].

### Analysis in FEM

The finite element method is a numerical analysis technique for obtaining approximate solution to a wide variety of engineering problems. In engineering problems there are some basic unknowns. If they are found, the behavior of the entire structure can be predicted. The basic unknowns or the field variable which are encountered in the engineering problems are displacement in solid mechanics [12]. The finite procedure reduces such unknowns to a finite number by dividing the solution region into small part called elements as shown in figure 6 and by expressing the unknown field variable in terms of assumed approximating functions within each element. The approximating functions are defined in terms of field variable specified called nodes or nodal point [13]. Thus in the finite element analysis the unknowns are field variables of the nodal points. Once this are found the field variable at any point can be found by using interpolation functions. The various step involved in the finite element analysis are

- Select suitable field variables and the elements.
- Discretize the continua.
- Select the interpolation function.
- Find the element properties.
- Assemble element properties to get global properties.
- Impose the boundary conditions.
- Solve the system equations to get the nodal unknowns.
- Make the additional calculation to get the required values [10], [11].

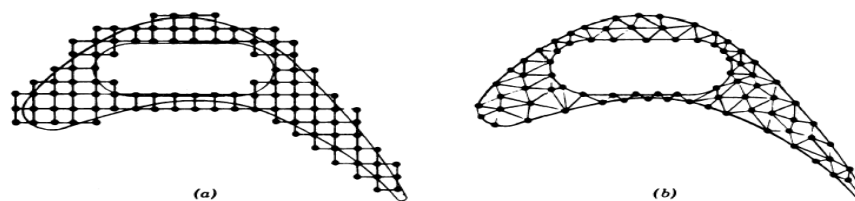


**Figure 6: Discretizations of Turbine Blade Profile**

### Element Types

The ANSYS element library contains more than 150 different element types. Each element type has a unique and prefix that identifies the element category: BEAM4, PLANE77, SOLID96, etc. The element type determines, among other things the degree of freedom set (which in turn implies the discipline-structural, thermal, magnetic, electric, quadrilateral, brick, etc.) [14].

### Solid 185 3D 8-Nodes Structural Solid Element

SOLID185 is used for 3-D modeling of solid structures. It is defined by eight nodes having three degrees of

freedom at each node as shown below in figure 7, translations in the nodal x, y, and z directions. The element has plasticity, hyper elasticity, stress stiffening, creep, large deflection, and large strain capabilities. It also has mixed formulation capability for simulating deformations of nearly incompressible elastoplastic materials, and fully incompressible hyper elastic materials[14].

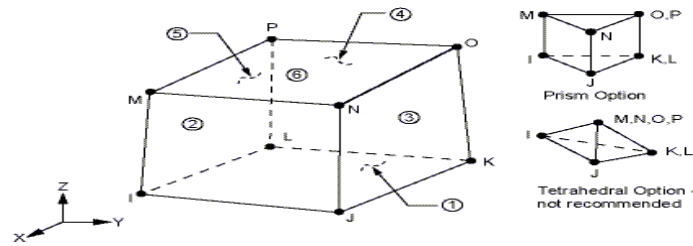


Figure 7: Solid 185 Structural Solid Geometry

**Element name** Solid 185

**Nodes** I, J, K, L, M, N, O, P

**Degrees of Freedom** UX, UY, UZ

**Real Constants** None

**Material Properties** EX, EY, EZ, PRXY, PRYZ, PRXZ (or NUXY, NUYZ, NUXZ), ALPX, ALPY, ALPZ (or CTEX, CTEY, CTEZ or THSX, THSY, THSZ), DENS, GXY, GYZ, GXZ, DAMP

**Surface Loads** Pressure

**Body Loads** Temperature

**Special Features** Plasticity, Hyper elasticity, Viscoelasticity, viscoplasticity, Elasticity, Other material, Stress stiffening, Large deflection, Large strain, Initial stress import and Nonlinear stabilization [14].

**Solid 70 3D 8-Nodes Thermal Solid Element**

Solid70 has a 3-D thermal conduction capability. The element has eight nodes with a single degree of freedom, temperature, at each node as shown as below in figure 8. The element is applicable to a 3-D, steady-state or transient thermal analysis. The element also can compensate for mass transport heat flow from a constant velocity field. If the model containing the conducting solid element is also to be analyzed structurally, the element should be replaced by an equivalent structural element (such as solid45). See solid90 for a similar thermal element, with mid-edge node capability. An option exists that allows the element to model nonlinear steady-state fluid flow through a porous medium. With this option, the thermal parameters are interpreted as analogous fluid flow parameters. For example, the temperature degree of freedom becomes equivalent to a pressure degree of freedom[14].

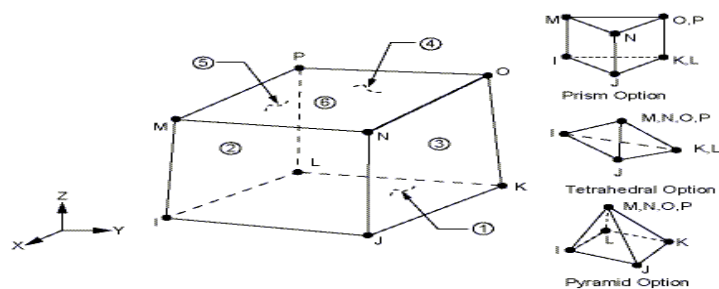


Figure 8: Solid-70 Geometry

**Element name** Solid 70

**Nodes** I, J, K, L, M, N, O, P

**Degrees of Freedom** TEMP

**Real Constants** Mass transport effects (KEYOPT (8) = 1): VX - X direction of mass transport velocity, VY - Y direction of mass transport velocity, VZ - Z direction of mass transport velocity

**Material Properties** KXX, KYY, KZZ, DENS, C, ENTH, VISC, MU

**Surface Loads** Convection or Heat Flux (but not both) and Radiation (using Lab = RDSF), Face 1 (J-I-L-K), face 2 (I-J-N-M), face 3 (J-K-O-N), Face 4 (K-L-P-O), face 5 (L-I-M-P), face 6 (M-N-O-P)

**Body Loads** Heat Generations

**Special Features** [14].

### Evaluation of Gas Forces on the Rotor Blades

Gas forces acting on the blades of the rotor in general have two components namely tangential ( $F_t$ ) and axial ( $F_a$ ). These forces result from the gas momentum changes and from pressure differences across the blades. These gas forces are evaluated by constructing velocity triangles at inlet and outlet of the rotor blades. The rotor blades considered for analysis are untwisted and same profile is taken throughout the length of the blade. If the gas forces are assumed to be distributed evenly then the resultant acts through the centroid of the area [1], [2].

### Evaluation of Gas Forces on the First Stage Rotor Blade

At the inlet of the first stage rotor blades,

Absolute flow angle  $\alpha = 23.85^\circ$

Absolute velocity  $V_1 = 462.21 \text{ m/s}$

The velocity triangles at inlet of first stage rotor blades were constructed as shown in figure 9.

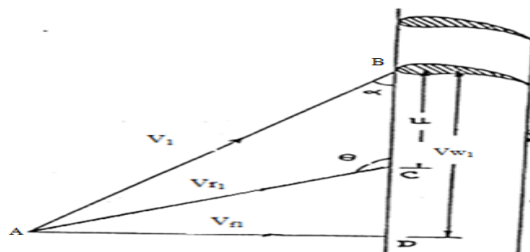


**Figure 9: Inlet Velocity Triangles of I-Stage Rotor Blades**

Diameter of blade mid span  $D = 1.3085 \text{ m}$

Design speed of turbine  $N = 3426 \text{ rpm}$

Peripheral speed of rotor blade at its mid span,  $U = \pi DN/60$

From the velocity triangles in figure 9 we get,

Whirl velocity  $V_{w1} = 422.74 \text{ m/s}$

Flow Velocity  $V_{f1} = 186.89 \text{ m/s}$



Relative velocity,  $V_{r1} = 265.09 \text{ m/s}$

Blade angle at inlet,  $\theta = 135.017^\circ$

At the exit of the first stage rotor blades,

Flow velocity,  $V_{f2} = 180.42 \text{ m/s}$

Relative flow angle,  $\Phi = 37.88^\circ$

The velocity triangles at the exit of the first stage rotor blades as were constructed as shown in figure 10.

From the velocity triangles in figure 10 we get,

Whirl velocity,  $V_{w2} = 2.805 \text{ m/s}$

Relative velocity,  $V_{r2} = 293.83 \text{ m/s}$

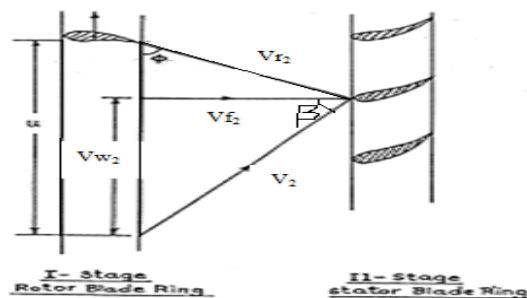


**Figure 10: Exit Velocity Triangles of I-Stage Rotor Blades**

The gas forces and power developed in the first stage rotor blades were evaluated using the equations that were used for first stage rotor blades.

Tangential force  $F_t = 248.199 \text{ Newton}$

Axial force  $F_a = 3.82 \text{ Newton}$ .

Power developed  $P = 6.991 \text{ mega watts}$ .

Centrifugal force  $F_c = 38038.73 \text{ Newton}$  [1], [2].

**Convective Heat Transfer Coefficients over the Blade Surfaces**

The flows over suction and pressure side of rotor blade as shown in figure 11.

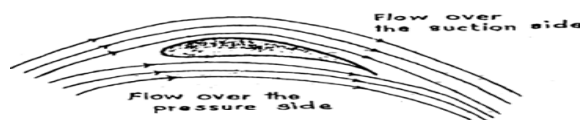


**Figure 11: Gas Flows over Suction and Pressure Side of Rotor Blade**

Convective Heat Transfer Coefficients on Suction side of Rotor Blades  $h_s = 379.92 \text{ w/m}^2 \text{ k}$ .

Convective Heat Transfer Coefficients on the Pressure side of rotor blade  $h_p = 284.95 \text{ w/m}^2 \text{ k}$  [1], [2],[15].

**Evaluation of Convective Heat Transfer Coefficient (hr)**

Convective Heat Transfer Coefficient (hr) on the Two Rectangular Faces at inlet and Exit of Rotor Blades as shown in figure 12.

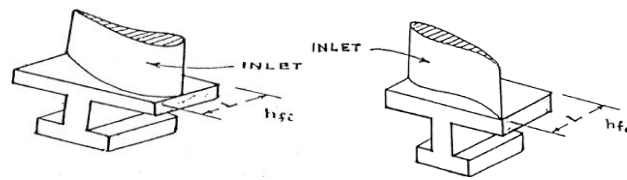


**Figure 12: Inlet and Exit of the Rotor Blade**

Convective heat transfer coefficients on the rectangular face at inlet  $h_{fi} = 231.195 \text{ w/m}^2 \text{ K}$ .

Convective heat transfer coefficients on the rectangular face at exist  $h_{fe} = 224.73 \text{ w/m}^2 \text{K}$  [1], [2],[15].

### Structural Analysis of a Gas Turbine Rotor Blade

Element Type 1: Solid 185 3D 8-nodes Structural Solid Element

Element type 2: Solid70 3D 8-nodes Thermal Solid Element

Young's Modulus of Elasticity (E)

Poisson ratio ( $\mu$ )

Density ( $\rho$ )

Coefficient of thermal expansion ( $\alpha$ )

The aero foil profile of the rotor blade was generated on the XY plane with the help of key points defined by the coordinates as shows in table 2. Then a number of splines were fitted through the key points. A rectangle of dimensions 49\*27 mm was generated as shown in figure 13, [14].

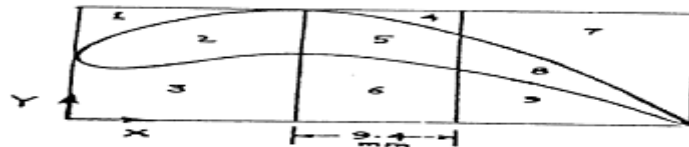


**Figure 13: Boundary of Aero Foil Section**

**Table 2: (Figure 13) List of Selected Key Point**

NO.	X	Y	NO.	X	Y
1	0.00	0.00	20	49	0.00
2	2.6	17.3	21	49	27.00
3	5.85	21	22	0.00	27.00
4	10	25	23	19.8	0.00
5	14.8	26.6	24	1.00	13.6
6	22.9	25.3	25	29.2	0.00
7	28	22.2	26	29.2	27.00
8	33.4	18.5	27	19.8	27.00
9	38	14.4	28	15.2	27.00
10	42	10.9	29	18.08	27.00
11	45.5	5.70	30	49.00	0.27E-1
12	49.00	0.00	31	48.90	0.288E-1
13	6.18	12.4	32	29.2	12.49
14	11.2	14.4	33	19.8	26.62
15	16.18	15.5	34	19.8	15.12
16	21.1	14.9	35	29.2	21.25
17	26	13.6	36	0.00	0.30E-1
18	38.2	8.77	37	19.8	0.30E-1
19	45	3.95	38	19.8	15.12

Using splines and lines 9 different areas were generated as volumes. In the shape and size option, the number of element edges along the lines surrounding the areas 1 to 9 was specified. In the attribute option element type 1 and material type 1 were assigned to the two areas. Areas 1 to m9 were extruded upwards in the positive Z direction through a height of 5mm. After extrusion, the rectangular block as shown as in figure 14 was generated.

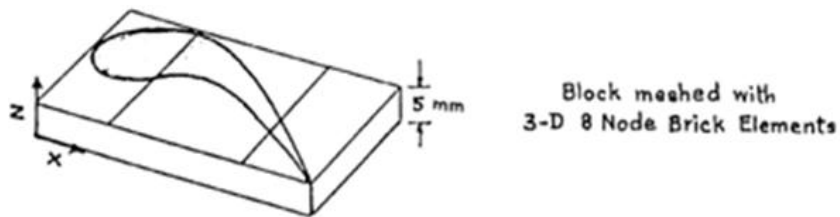


Figure 14: Turbine Rotor Block

Again using the extrusion option, the shaded area as shown in figure 15 was extruded upwards through the blade height (117 mm) along the positive Z direction, Areas 4,5,6 were extruded downwards along the negative direction through a distance 14.5 mm. The model was generated as shown in figure 22 by use in the preprocessor of ANSYS12.0 [14].

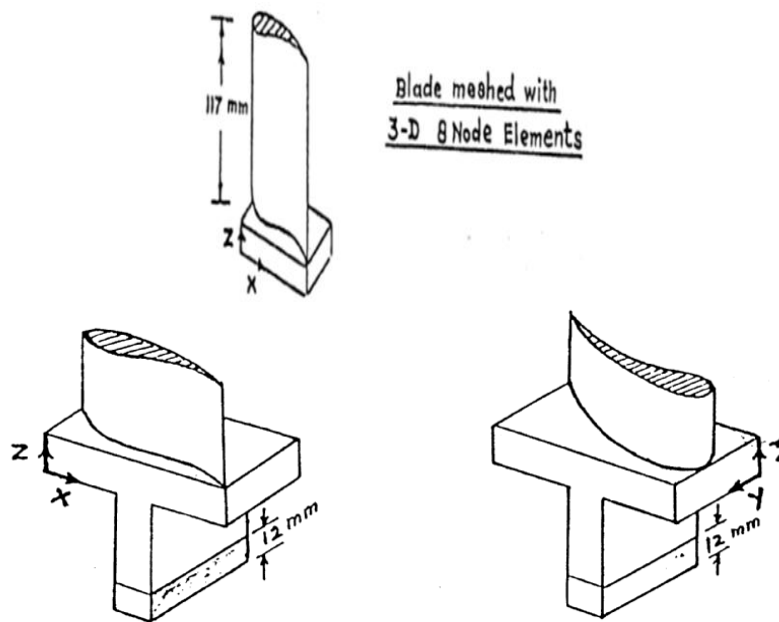


Figure 15: Volume of Rotor Blade

The shaded areas shown below in figure 16 were extruded along the X-direction through a distance of 3.8 mm using the mesh option all the areas were meshed with Brick 8-node 185 elements as shown in figure 23[14].

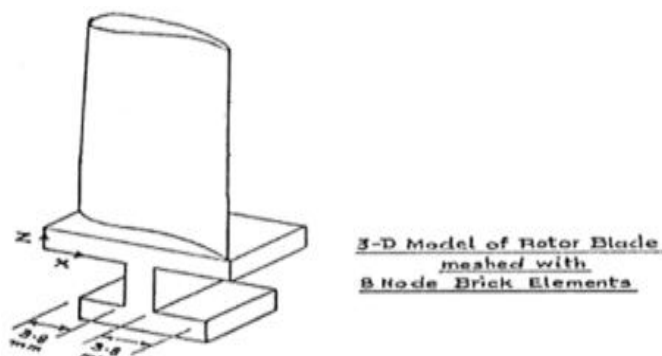
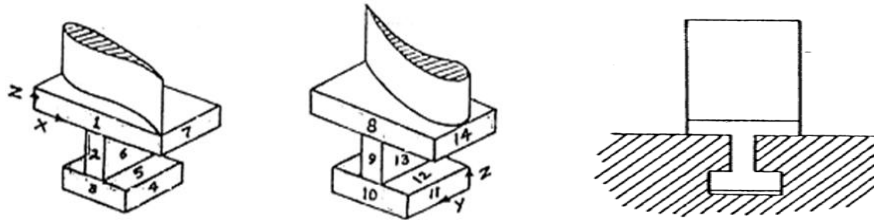


Figure 16: 3-D Model of Rotor Blade

**Structural Boundary Conditions to Be Applied on the Rotor Blade Model**

Two structural boundary conditions namely displacement and force were applied on the rotor blade model as shown in figure 17.



**Figure 17: Structural Boundary Conditions on Rotor Blade**

$U_x = 0$  for areas 4,5,6,7 and 11,12,13,14

$U_y = 0$  for areas 1, 2, 3 and 8,9,10

$U_z = 0$  for areas 5 and 12

U represents displacement and suffix X, Y; Z represents the direction in which the displacement was constrained.

In the solution part of Ansys the blade forces namely tangential, axial and centrifugal were applied on the node located at the centroid of the blade as shown in figure 18.

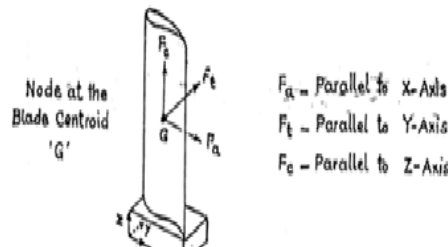


**Figure 18: Static Loading on Rotor Blade**

**Thermal Boundary Conditions Applied on the Rotor Blade Model**

Heat flux = 0 from areas 1, 2... to 16.

Areas 1, 2, 3 and 8,9,10 come in contact with similar areas on the adjacent rotor blades as shown in figure 17. Hence due to symmetry boundary conditions, these areas are assumed to be insulated. Areas 4, 5, 6 and 11,12,13,15 on account of their small dimensions are assumed to be insulated. In the convective boundary condition, the convective heat transfer coefficient (h) and temperature of surrounding gases (T) have to be specified on the areas subjected to convection as shown below in figure 19[1],[15].

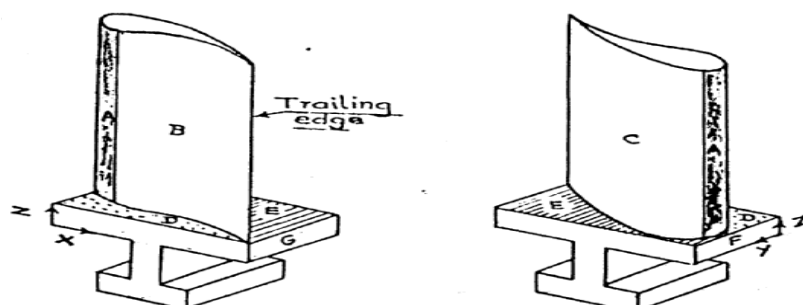


**Figure 19: Thermal Boundary Conditions**

## RESULTS AND DISCUSSIONS

### Structural Analysis

#### Case1: Von Mises Stress Of Titanium, Aluminum2024 and Stainless Steel Alloys

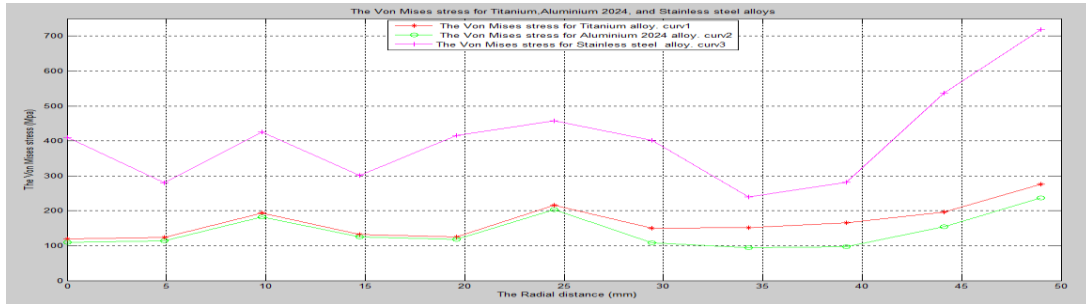


**Figure 20: The Von Mises Stresses (MPa) of Titanium, Stainless Steel and Aluminum 2024 Alloys**

Figure 20 shows that variation of stresses along the radial distance. It is observed that the stress is varying as the radial distance increases. The maximum stresses are observed to be 719.075 MPa for stainless steel alloy at a distance of 49 mm and the minimum stresses are observed to be 94.8706MPa for Aluminum 2024 Alloy at a distance of 34.3 mm as shown in figure 24, 25 and 26.

#### Case2: Resultant Deformation of Titanium, Aluminium 2024 and Stainless Steel Alloys

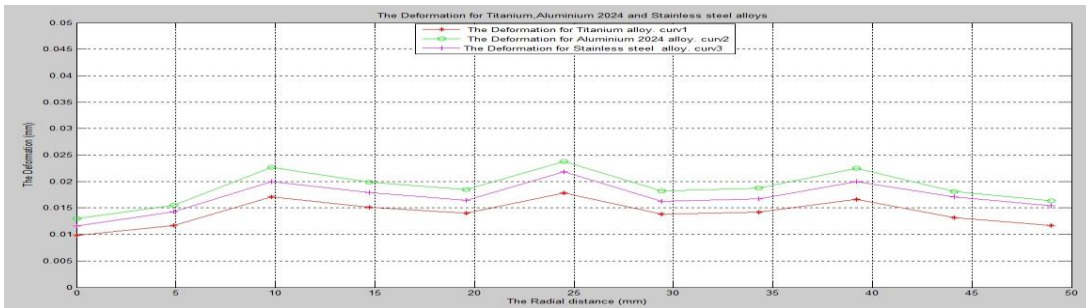


**Figure 21: Deformation Variations (mm) of Titanium, Stainless Steel and Aluminum 2024 Alloys**

Figure 21 shows the variation of deformation along the radial distance .It is observed that the deformation is varying as the radial distance increases and maximum is 0.023821mm for the Aluminum 2024 Alloys and minimum is 0.00978284 mm for the Titanium alloys as shown in figure 27, 28 and 29.

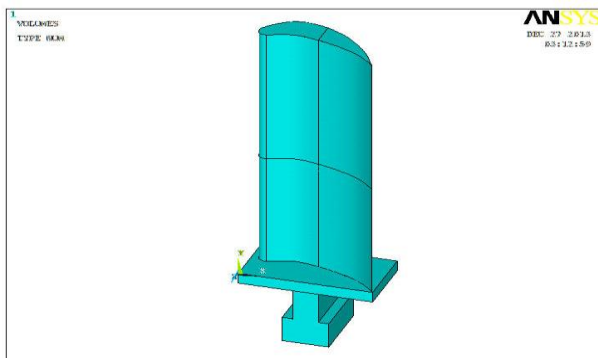


**Figure 22: Solid Model of Gas Turbine Blade**

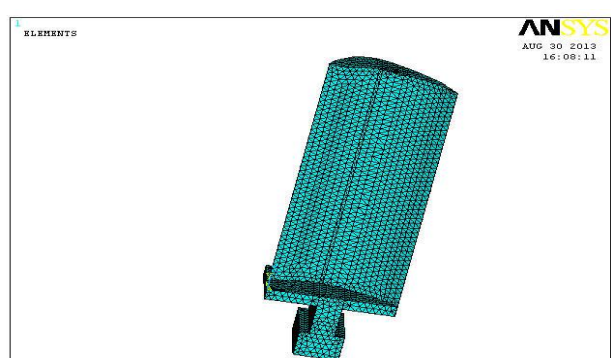


**Figure 23: Finite Element Modal Free Mesh**

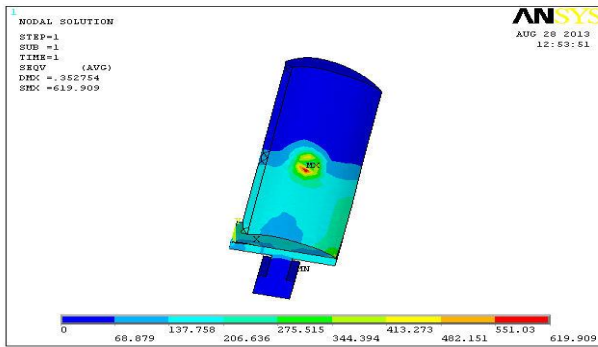


Figure 24: Von Mises Stress of Titanium Alloy, MPa

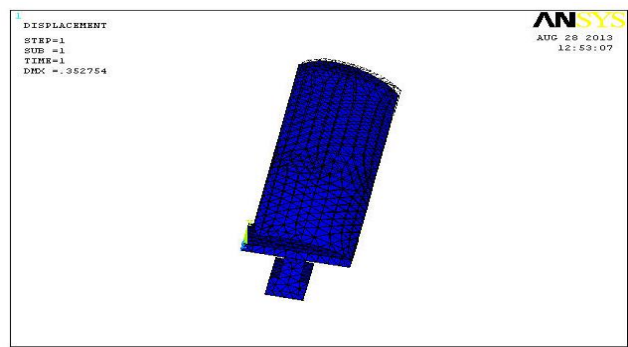


Figure 27: Resultant Deformation of Titanium Alloy, mm

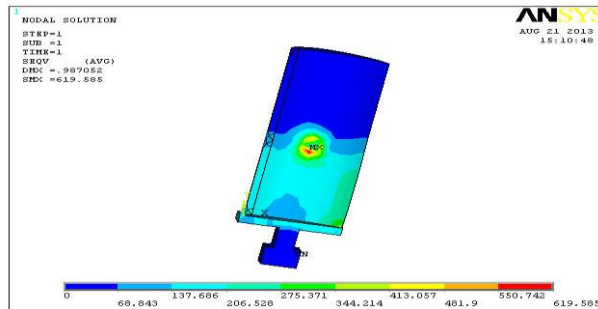


Figure 25: Von Mises Stress of Aluminum 2024 Alloy, MPa

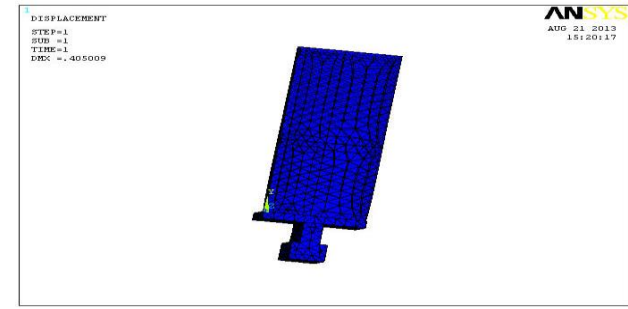


Figure 28: Resultant Deformation of Stainless Steel Alloy, mm

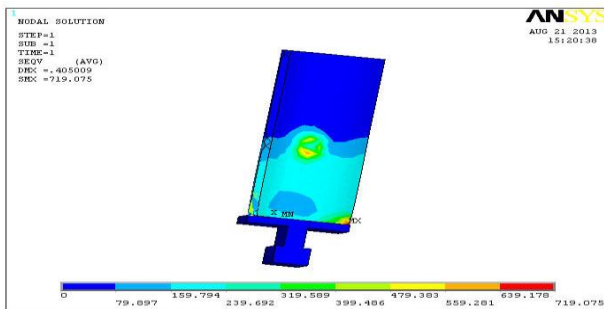


Figure 26: Von Mises Stress of Stainless Steel Alloy, MPa

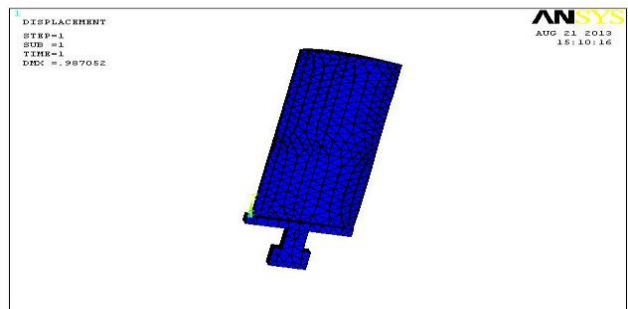


Figure 29: Resultant Deformation of Aluminum 2024 Alloy, mm

**THERMAL ANALYSIS**

**Case1: Temperature Distribution of Titanium, Aluminum2024 and Stainless Steel Alloys**

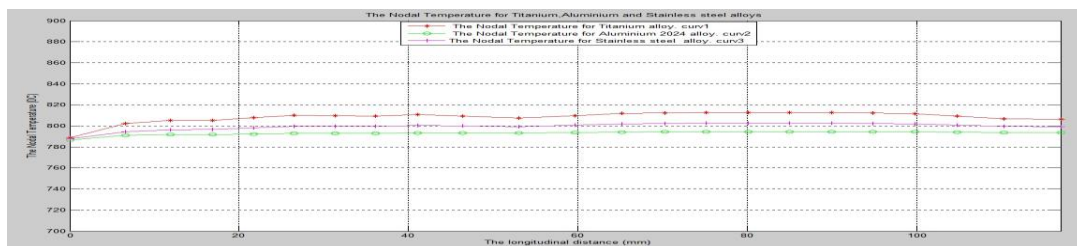
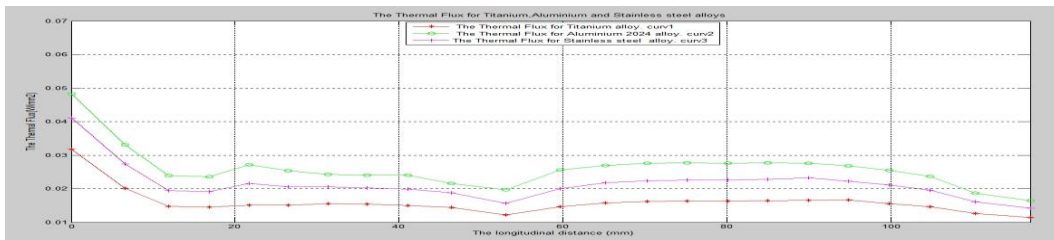


Figure 30: Variation of Nodal Temperature with Longitudinal Distance of Titanium, Stainless Steel and Aluminum 2024 Alloys

Figure 30 shows the variation of resultant nodal temperature along the longitudinal distance. It is observed that the variation is nonlinear and maximum temperature is observed to be 812.78 °C for titanium alloy and minimum temperature is 786.674 °C for Aluminum 2024 alloy as shown in figure 33, 34 and 35.

**Case 2: Thermal Flux of Titanium, Aluminum2024 and Stainless Steel Alloys**



**Figure 31: The Thermal Flux with Longitudinal Distance of Titanium, Stainless Steel and Aluminum 2024 Alloys**

Figure 31 shows the variation of resultant thermal flux along the longitudinal distance .It is observed that the variation are nonlinear and maximum temperature is observed that  $0.0482527\text{W/mm}^2$  for Aluminum 2024 alloy and the minimum temperature is  $0.0114133\text{ W/mm}^2$  for Titanium Alloy as shown in figure 36,37 and 38.

**Case 3: Thermal Gradient of Titanium, Aluminum2024 and Stainless Steel Alloys**

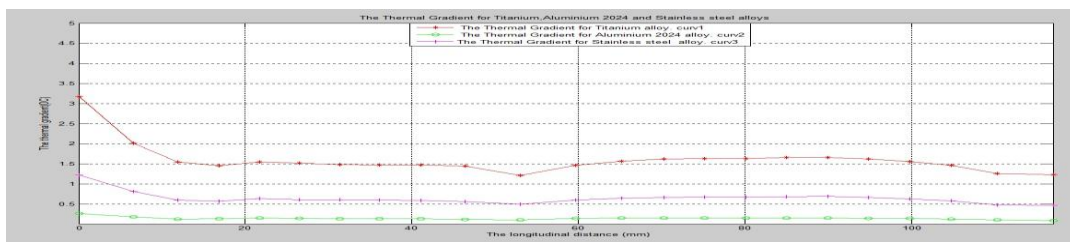


**Figure 32: Thermal Gradient Vector with Longitudinal Distance of Titanium, Stainless Steel and Aluminum 2024 Alloys**

Figure 32 shows the variation of resultant thermal gradient along the longitudinal distance. It is observed that the variation is nonlinear and maximum temperature is observed to be  $3.175\text{ }^{\circ}\text{C}$  for Titanium Alloy and minimum temperature is  $0.0910778\text{ }^{\circ}\text{C}$  for Aluminum 2024 Alloy as shown in figure 39,40 and 41.

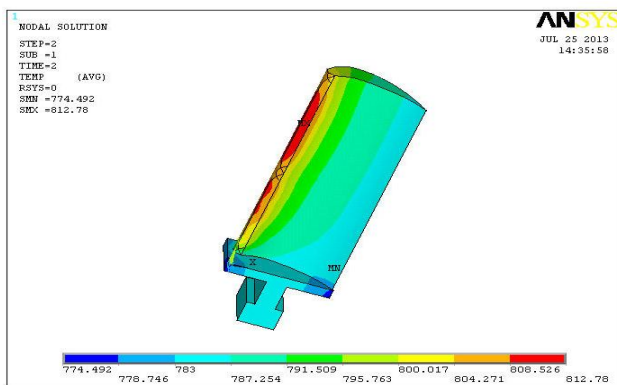


**Figure 33: Temperature Distribution of Titanium Alloy, 0C**

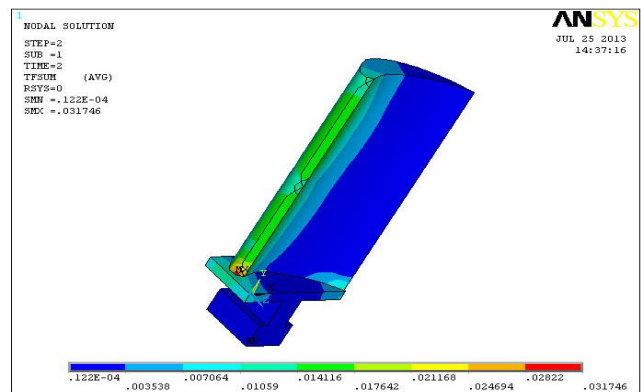


**Figure 36: Thermal Flux Vector Sum of Titanium Alloy, W/mm2**

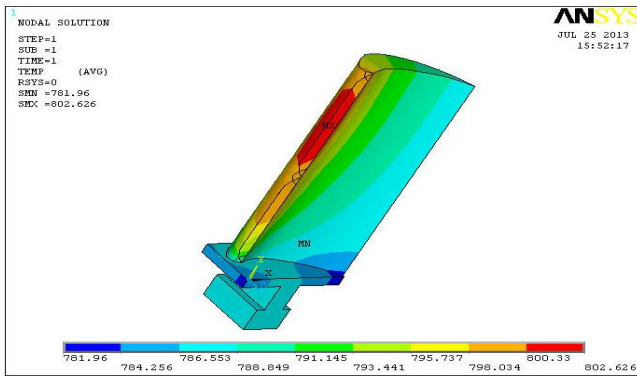


Figure 34: Temperature Distribution of Stainless Steel Alloy, 0C

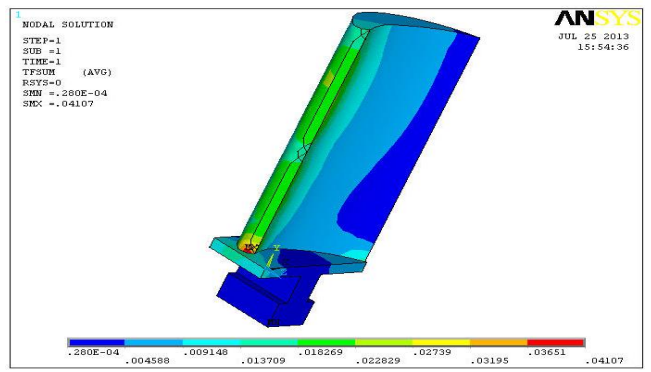


Figure 37: Thermal Flux Vector Sum of Stainless Steel Alloy, W/mm2

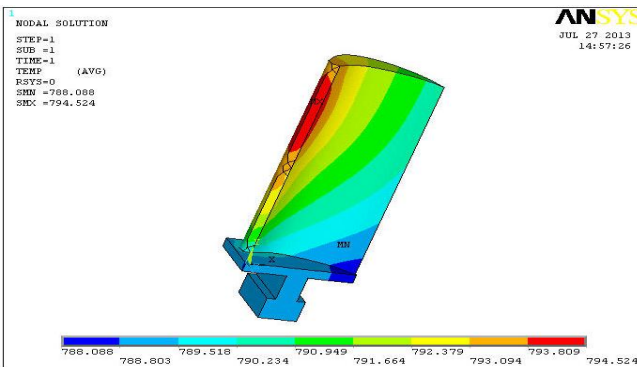


Figure 35: Temperature Distribution of Aluminum 2024 Alloy, 0C

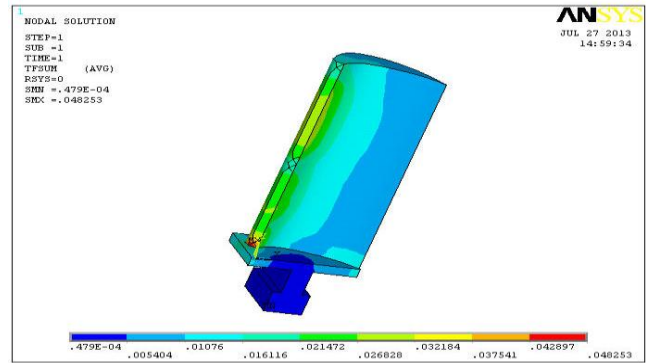


Figure 38: Thermal Flux Vector Sum of Aluminum 2024 Alloy W/mm2

**MODAL ANALYSIS**

**Case1: Modal Analysis of Titanium Alloy Rotor Blade**

The mode shape of rotor blade made of titanium alloy as shown in figure 42, 43 and 44. It is observed that the maximum resultant deformation (relative) is 1.149 at 162 Hz natural frequency.

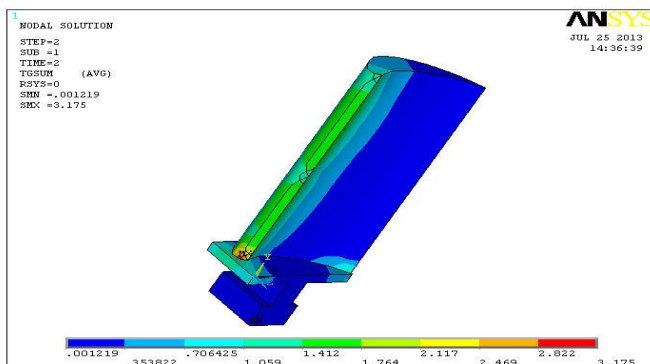


Figure 39: Thermal Gradient of Titanium Alloy, 0C

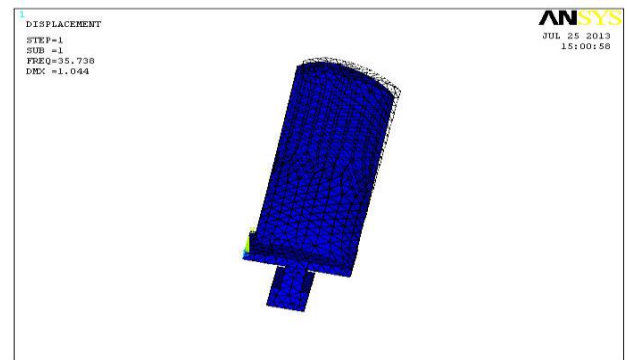


Figure 42: 1<sup>st</sup> Mode Shape of Titanium Alloy Rotor Blade



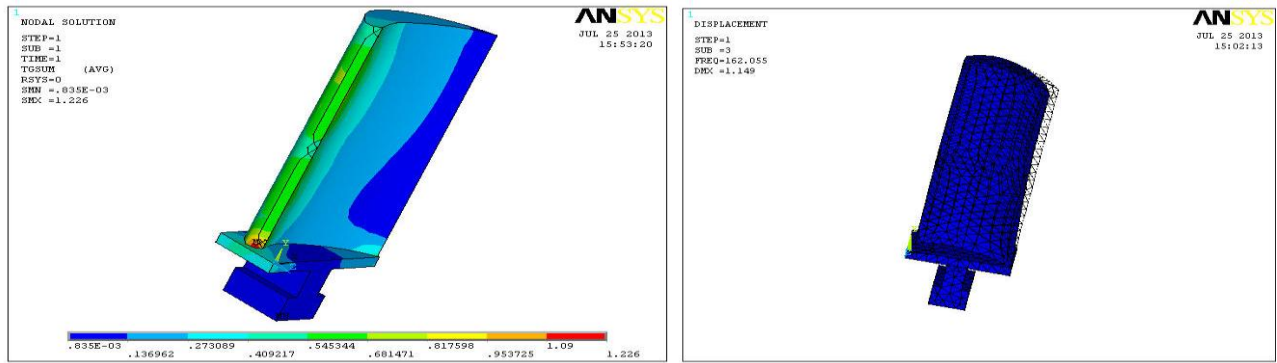


Figure 40: Thermal Gradient of Stainless Steel Alloy, 0C Figure 43: 2<sup>nd</sup> Mode Shape of Titanium Alloy Rotor Blade

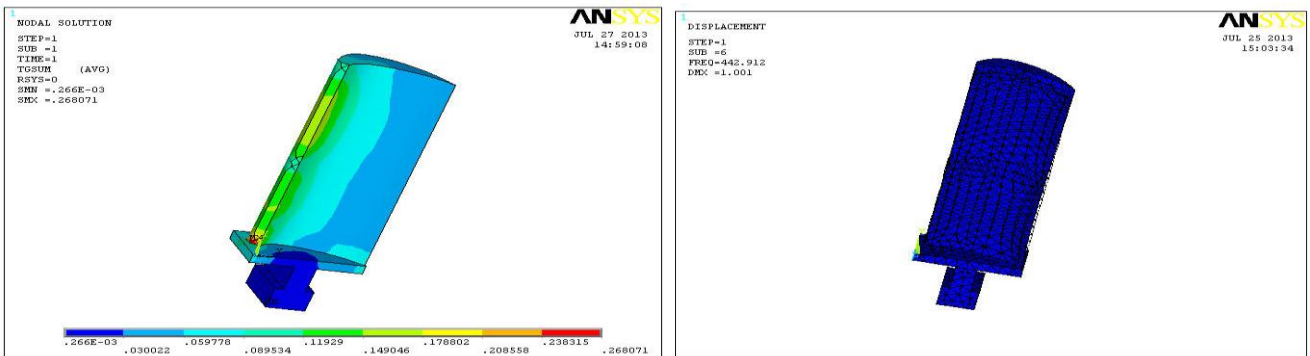


Figure 41: Thermal Gradient of Aluminum 2024 Alloy, 0 Figure 44: 3<sup>rd</sup> Mode Shape of Titanium Alloy Rotor Blade

**Case2: Modal Analysis of Stainless Steel Alloy Rotor Blade**

The mode shape of rotor blade made of stainless steel alloy as shown in figure 45, 46 and 47. It is observed that the maximum resultant deformation (relative) is 1.149 at 124 Hz natural frequency.

**Case3: Modal Analysis of Aluminum 2024 Alloy Rotor Blade**

The mode shape of rotor blade made of Aluminum 2024 alloy as shown in figure 48, 49 and 50. It is observed that the maximum resultant deformation (relative) is 1.149 at 127 Hz natural frequency.

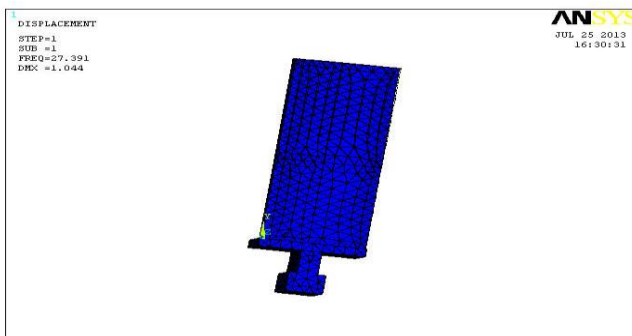


Figure 45: 1<sup>st</sup> Mode Shape of Stainless Steel Alloy, Rotor Blade

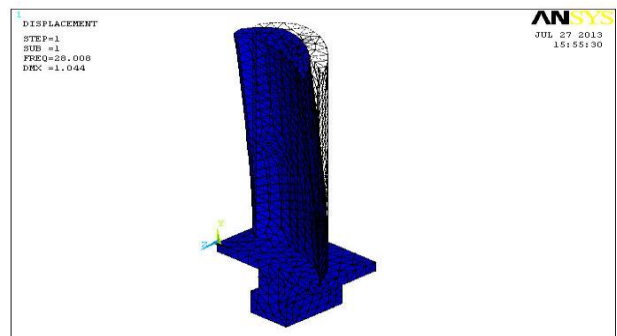


Figure 48: 1<sup>st</sup> Mode Shape of Aluminum2024 Alloy, Rotor Blade

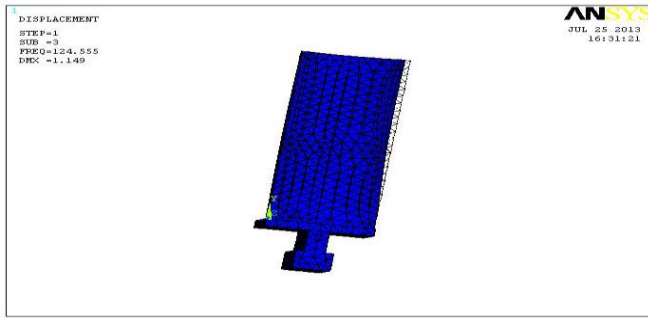


Figure 46 2<sup>nd</sup> Mode Shape of Stainless Steel Alloy, Rotor Blade

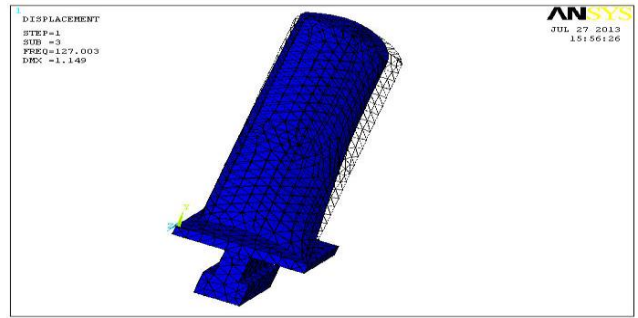


Figure 49: 2<sup>nd</sup> Mode Shape of Aluminum 2024 Alloy, Rotor Blade

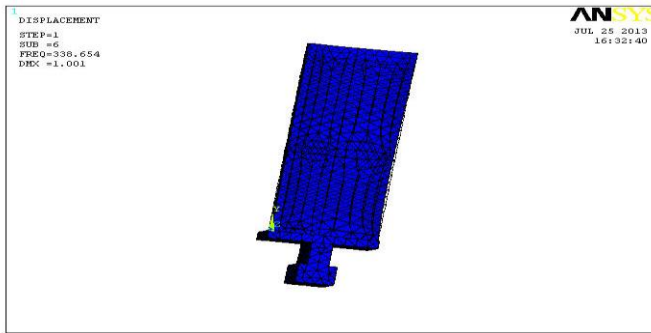


Figure 47: Shows 3<sup>rd</sup> Mode Shape of Stainless Steel Alloy, Rotor Blade

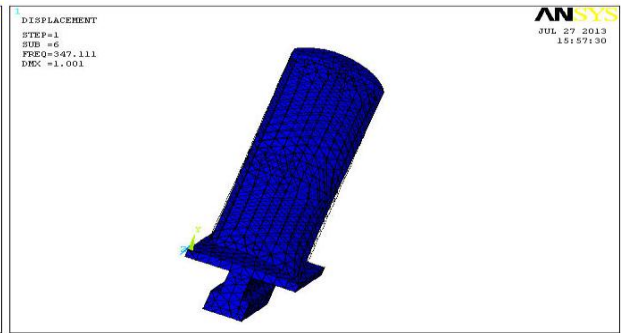


Figure 50: Shows 3<sup>rd</sup> Mode Shape of Aluminum 2024 Alloy, Rotor Blade

**RESULTS AND DISCUSSIONS**

**Table 3: Structural and Thermal Analysis**

Material type	VonMises Stress (MPa)	Deformation (mm)	Nodal Temperature (°C)	Thermal Flux (W/mm <sup>2</sup> )	Thermal Gradient (°C)
Titanium alloy	619.909	0.352754	812.78	0.031746	3.175
Stainless steel alloy	719.075	0.405009	802.626	0.04107	1.226
Aluminum 2024 alloy	619.585	0.987052	794.524	0.048253	0.268071

**Modal Analysis**

**Table 4**

Mode shape	Titanium alloy	Stainless steel alloy	Aluminum 2024 alloy
Mode1	35.738	27.391	28.008
Mode2	162.055	124.555	127.003
Mode3	442.912	338.654	347.111

**CONCLUSIONS**

The finite element analysis of gas turbine rotor blade is carried out using 8 noded brick element. The static and thermal analysis is carried out. The temperature has a significant effect on the overall stresses in the turbine blades. Maximum temperatures are observed at the blade tip section and minimum temperature variations at the root of the blade. Temperature distribution is almost uniform at the maximum curvature region along blade profile. Temperature is linearly decreasing from the tip of the blade to the root of the blade section. For all the materials the temperature maximum observed is varying between 794°C to 812°C. Maximum stress induced is within safe limits for all the materials except aluminum. The modal analysis reveals that the fundamental frequency of titanium alloy is highest (35Hz) as compared all other materials. Hence resonance delay for this hence dynamically more stable.

## REFERENCES

1. **R.Yadav,(1993)**. Steam and Gas turbine, *Central Publishing House, Allahabad*.
2. **Meherwanp.Boyce, (2012)**.Gas turbine engineering,fourth edition,*Elsevier Inc, United States of America*.
3. **Claire Soares,(2008)**.gas turbine a hand book of air ,land and sea applications ,*Elsevier Inc, united states of america*.
4. **Nageswara Rao Muktinutalapati, (2011)**.Application in Gas Turbines, *Materials Science and Engineering*, Vol.88, pp11-19, ISSN 0921-5093.
5. **J. C. Han, S. Dutta, and S.V. Ekkad, (2000)**.Gas Turbine Heat Transfer and Cooling Technology, Taylor &Francis, Inc, New York, ISBN # 1-56032-841-X, 646 pages.
6. **A.John. Sedriks, (1979)**.Corrosion of Stainless Steels, *Original from the University of California*,ISBN 0471050113, 9780471050117, 282 pages.
7. **M. Niinomi, (1998)**.Mechanical properties of biomedical titanium alloys, *Mater. Sci. Engng*,A 243 pp 231–236.
8. **K. Mahadevan and K.Balaveera reddy, (1984)**.Design data hand book for mechanical engineering, *CBS Publ, second Edition*, 434 pages.
9. **S. S. Rao, (1999)**.The Finite Element method in Engineering, BH Publications New Delhi, 3rd Edition.
10. **O. C.Zeinkiewicz, (1992)**.The Finite Element method in Engineering Science, *Tata McGraw Hill*, 2nd Edition.
11. **O. P. Gupta, (1999)**.Finite and Boundary element methods in Engineering, *Oxford and IBH publishing company Pvt .Ltd. New Delhi*.
12. **C. S. Krishnamoorthy, (1987)**.Finite Element Analysis, Theory and Programming, *Tata McGraw-Hill Publishing Company Ltd., New Delhi*.
13. **P. Ravinder Reddy, (1999)**.CADA Course Book, *AICTE-ISTE sponsored programme*.
14. **ANSYS Theory Manual**, ANSYS/ inc.U.S.A, *Version 12.0*.
15. **Sadikkakac and Yaman Yener, (1995)**.convective heat transfer, second edition, *CRC PRESS LLC, UNITED STATE of America*.

## AUTHOR'S DETAILS



**Mr. Ahmed Abdulhussein Jabbar** Received his bachelor of Mechanical Engineering department, College of Engineering, AL- Mustansiriya University Iraq in 2011. He is Pursing M.Tech Machine Design engineering, Mechanical Engineering Department Shepherd School of Engineering and Technology, Sam Higginbottom Institute of Agriculture, Technology and Sciences, Allahabad, India. He has experience for one year in Project implementation of networks streams

in misan .He knows to work on Analytical and Design Software such as AutoCAD from Autodesk, ANSYS, CFD, ICEM, GAMBIT, FLUENT, CFX, Hypermesh and Professional certificate in Mechanical CADD (CATIA, Pro.E and Solidworks).



**Dr A. K. Rai** is born in 1977, Distt. Ballia (Uttar Pradesh) India. He received his M.Tech Degree from MNNIT Allahabad in Design of Process Machines and Ph.D. from SHIATS- DU Allahabad in 2011. He has been in GBPUAT Pant nagar from 2003 to 2005. He is Joined SHIATS-DU Allahabad as assistant Professor in 2005. He has published more than 20 papers in international journals.



**Prof. (Dr) P. Ravinder Reddy** is born on August 12th 1965, graduated in B.Tech Mechanical Engineering from Kakatiya University (1987) Warangal, M.E Engineering Design from PSG college of Technology, Coimbatore (1991) and Ph.D from Osmania University in 2001. He has 25 years of Teaching, Industrial and Research experience. He published over 175 technical and research papers in various international and national journals and conferences. He has guided 11 Ph.Ds. He has organized 23 workshops, 2 international conferences and delivered 93 keynote and invited talks. Was a chief and principal investigator for 13 research and 27 industrial consultancy sponsored projects. He is a recipient of **Raja Rambapu Patil National award** for promising Engineering Teacher by ISTE for the year 2000 in recognition of his outstanding contribution in the area of Engineering and Technology, **“Engineer of the year Award-2004”** for his outstanding contribution in Academics and research by the Govt. of Andhra Pradesh and Institution of Engineers (India), AP State Centre on 15th September 2004 on the occasion of 37th Engineer’s Day, **Best Technical Paper Award** in the year Dec. 2008 in Industrial Application titled “Online quality monitoring welding & weld upset in resistance projection welding process”, in Journal of Non-Destructive Testing & Evaluation, the official journal of ISNT during the year 2007 by National Governing Council of Indian Society for Non Destructive Testing.



**Mr. Mahmood Hasan Dakhil** Received his bachelor of Mechanical Engineering department, College of Engineering, THI-QAR University Iraq in 2010. He is Pursing M.Tech Machine Design engineering, Mechanical Engineering Department Shepherd School of Engineering and Technology, Sam Higginbottom Institute of Agriculture,

Technology and Sciences, Allahabad, India. He has experience for Project implementation of networks streams in Misan,AzharAlnahjCompany& Al-Hassnawi Company. He knows to work on Analytical and Design Software such as AutoCAD&Inventor from Autodesk,ANSYS,CFD,ICEM,GAMBIT,FLUENT,CFX,Hypermesh and Professional certificate in Mechanical CADD(CATIA,Pro.E and Solidworks).

